GEOPHYSICAL RESEARCH LETTERS, VOL. 37, L08103, doi:10.1029/2009GL041971, 2010

Multiple overshoot and rebound of a bursty bulk flow

E. V. Panov,[1,2] R. Nakamura,[1] W. Baumjohann,[1] V. Angelopoulos,[3] A. A. Petrukovich,[4] A. Retinò,[1] M. Volwerk,[1] T. Takada,[5] K.-H. Glassmeier,[6,7] J. P. McFadden,[8] and D. Larson[8]

Received 1 December 2009; revised 11 February 2010; accepted 4 March 2010; published 20 April 2010.

[1] Chen and Wolf (1999) used a thin-filament theory to construct a 2D model of a bursty bulk flow (BBF) motion inside the plasma sheet. The modeling revealed that the low-entropy filament overshoots its equilibrium position and executes a heavily damped oscillation about that position. In this letter we demonstrate, for the first time, the multiple overshoot and rebound of a BBF observed by the five THEMIS probes on 17 March 2008 just after 10:22 UT. We found that the BBF oscillatory braking was accompanied by interlaced enhancements and depletions of radial pressure gradients. The earthward and tailward flow bursts caused formation of vortices with opposite sense of rotation. **Citation:** Panov, E. V., et al. (2010), Multiple overshoot and rebound of a bursty bulk flow, *Geophys. Res. Lett.*, *37*, L08103, doi:10.1029/2009GL041971.

1. Introduction

[2] Bursty bulk flows (BBFs)—fast plasma flows inside the plasma sheet [*Baumjohann et al.*, 1990; *Angelopoulos et al.*, 1992, 1994]—are often associated with substorms [*Baumjohann et al.*, 1991, 1999]. BBFs occur in very localized channels up to 2–3 Re wide [*Angelopoulos et al.*, 1996; *Sergeev et al.*, 1996; *Nakamura et al.*, 2004]. At around 10 Re, BBFs are suddenly decelerated by the dominant dipolar magnetic field [*Hesse and Birn*, 1991; *Shiokawa et al.*, 1997], where pressure gradients are piled up. The BBFs are also drivers of MHD waves in the magnetotail [*Volwerk et al.*, 2004].

[3] Observations and theory [*Goertz and Baumjohann*, 1991; *Chen and Wolf*, 1999; *Birn et al.*, 2004] have suggested that BBFs can be thought of as thin filaments inside the plasma sheet with entropy that is substantially lower than that of the surrounding plasma, resulting in earthward acceleration by the plasma buoyancy force. MHD modeling [*Birn et al.*, 2004] has predicted that the interaction of an incident flow in the plasma sheet with dipolar field lines of the Earth's magnetic field would result in flow deflection and formation of plasma vortices. Indeed, recent THEMIS observations have indicated signatures of vortical plasma motion in the near-Earth plasma sheet [*Keika et al.*, 2009; *Keiling et al.*, 2009; *Panov et al.*, 2010].

[4] *Chen and Wolf* [1999] predicted that the earthward accelerated BBF overshoots its equilibrium position and executes a heavily damped oscillation about that position. Based on THEMIS observations [*Angelopoulos*, 2008] on 17 March 2008 just after 10:22 UT, we demonstrate for the first time the multiple overshoot and rebound of a BBF. We find that while the earthward BBF overshootings are accompanied by enhanced radial pressure gradients, these gradients are depleted during the tailward rebounds of the BBF. In addition we show that changes of the flow burst propagation direction from earthward to tailward reversed the sense of rotation of the vortices on the two sides of the BBF.

2. Observations

[5] On 17 March 2008 at 10:25 UT the five THEMIS spacecraft were located between 22:00 and 23:00 hours MLT, and covered radial distances between 8 Re and 14 Re: P1 (red) at (−12.688, 3.297, −0.215) Re, P2 (green) at (−11.068, 2.716, −1.184) Re, P3 (cyan) at (−9.660, 2.095, −1.295) Re, P4 (blue) at (−10.242, 3.340, −1.599) Re and P5 (magenta) at (−8.502, 4.502, −1.891) Re in the GSM frame of reference.

[6] We use 128 Hz resolution magnetic field data from the fluxgate magnetometers (FGM) [*Auster et al.*, 2008] and sampled ion and electron distribution functions once every 3 seconds for particles with energies less than 30 keV from the Electrostatic Analyzers (ESA) [*McFadden et al.*, 2008] and from the Solid State Telescopes (SST) for particles with energies more than 30 keV. We use the combined ESA and SST measurements to improve the quality of the ion moments.

[7] Figure 1 shows data from the five spacecraft during the BBF event. They are plotted, from top to bottom, in the sequence of the BBF encounter by the spacecraft: P1, P2, P4, P3, and P5. Figure 1 (top) shows the *X*- and *Y*-GSM components, and the total ion bulk velocity (see legend for color coding). The left thick black line in Figure 1 indicates BBF onset for the five spacecraft. Later on, the velocity components executed a damped oscillation till about 10:32 UT.

[8] Figure 1 (bottom) shows the magnetic field measurements. Because B_Y was always the minor component, we

[1]Space Research Institute, Austrian Academy of Sciences, Graz, Austria.
[2]On leave from Space Research Institute, Russian Academy of Sciences, Moscow, Russia.
[3]Institute of Geophysics and Planetary Physics, University of California, Los Angeles, California, USA.
[4]Space Research Institute, Russian Academy of Sciences, Moscow, Russia.
[5]Institute of Space and Astronautical Science, JAXA, Sagamihara, Japan.
[6]Institut für Geophysik und Extraterrestrische Physik, Technische Universität Braunschweig, Braunschweig, Germany.
[7]Max-Planck-Institute for Solar System Research, Katlenburg-Lindau, Germany.
[8]Space Science Laboratory, University of California, Berkeley, California, USA.

0094-8276/10/2009GL041971

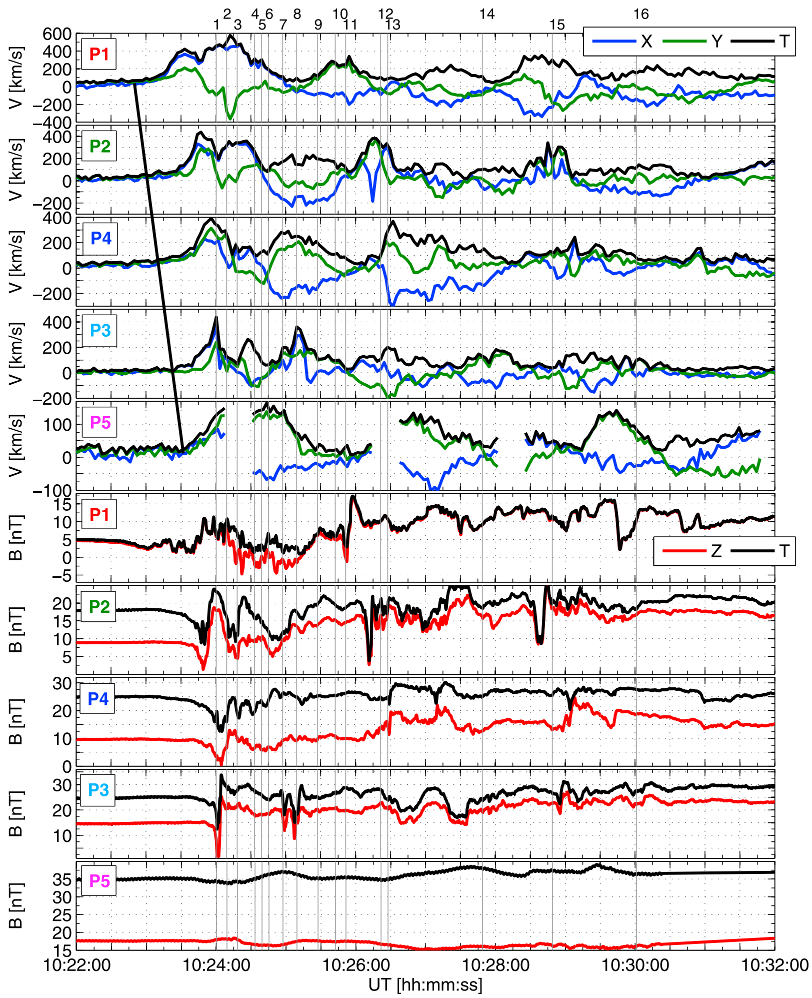

Figure 1. (top) Velocity and (bottom) magnetic field GSM-components and magnitudes from five THEMIS spacecraft on 17 March 2008 between 10:22 and 10:32 UT. See legends for color coding.

show only B_Z and the total magnetic field components. One can see that the spacecraft P1, P2, P3, and P4 observed stronger magnetic field fluctuations than spacecraft P5. P1, P2, P3, and P4 were located at nearly the same MLT, whereas P5 was about 1.5 hour MLT duskward from the other spacecraft.

[9] Figure 2 demonstrates the relationship between the oscillatory flows and the changes in the radial pressure gradient observed at the MLT of P1, P2, P3, and P4 spacecraft during the BBF event. Since the ESA detector did not provide full coverage of the ion energies in the plasma sheet, we use the sum of the ion density from ESA and SST spectrometers, which was in a good agreement with the electron density (not shown here).

[10] Figure 2a shows the entropy of the local flux tube PV^{γ}, for which the flux tube volume V was calculated using formula (6) of *Wolf et al.* [2006]. The formula assumes an inverse entropy dependence on the B_Z-component of the magnetic field. We use the polytropic index $\gamma = 5/3$ [*Goertz and Baumjohann*, 1991]. One can see that the region on the forefront of the BBF (between 10:23 and 10:24 UT), is associated with higher entropies. Further, the entropy drops indicating presence of a bubble at the positions of P1, P2, P3, and P4, around the times denoted by the black vertical lines 1 and 3. After the entropy minima observations by P1, P2, P3, and P4 the entropy enhanced again. The entropy remained nearly unchanged at the position of P5, indicating that the bubble has probably reached the shortest distance to the Earth not touching P5, and bounced then tailward. Between 10:25 UT and 10:32 UT the entropy traces exhibit unclear fluctuations reaching a stable level around 10:32 UT. The final entropy appeared to be lower than at 10:22 UT.

[11] In Figure 2b the sum of the plasma and the magnetic pressure is depicted. One can see from P1, P2, and P3 data that the total pressure maximum moves earthward (between 10:23:30 and 10:24:00 UT). Figure 2c shows the radial pressure gradient $\delta P/\delta R$ based on differences in the sum of the plasma and the magnetic pressure between P3 and P2 (solid line), and between P3 and P1 (dashed line). For the sake of better visibility we suppressed the high-frequency fluctuations in $\delta P/\delta R$ by averaging its value over 45-second-long window, sliding with 3-second step (one spacecraft spin). The two traces show similar signatures. Around vertical line 2 at 10:24:09 UT one can see an enhancement in $\delta P/\delta R$ (Maximum 1), which is associated with the arrival of the bubble (compare with Figure 2a). Later on, after 10:24:57 UT the pressure gradient depleted (Minimum 1). Since the second entropy enhancement is associated with the first depletion of

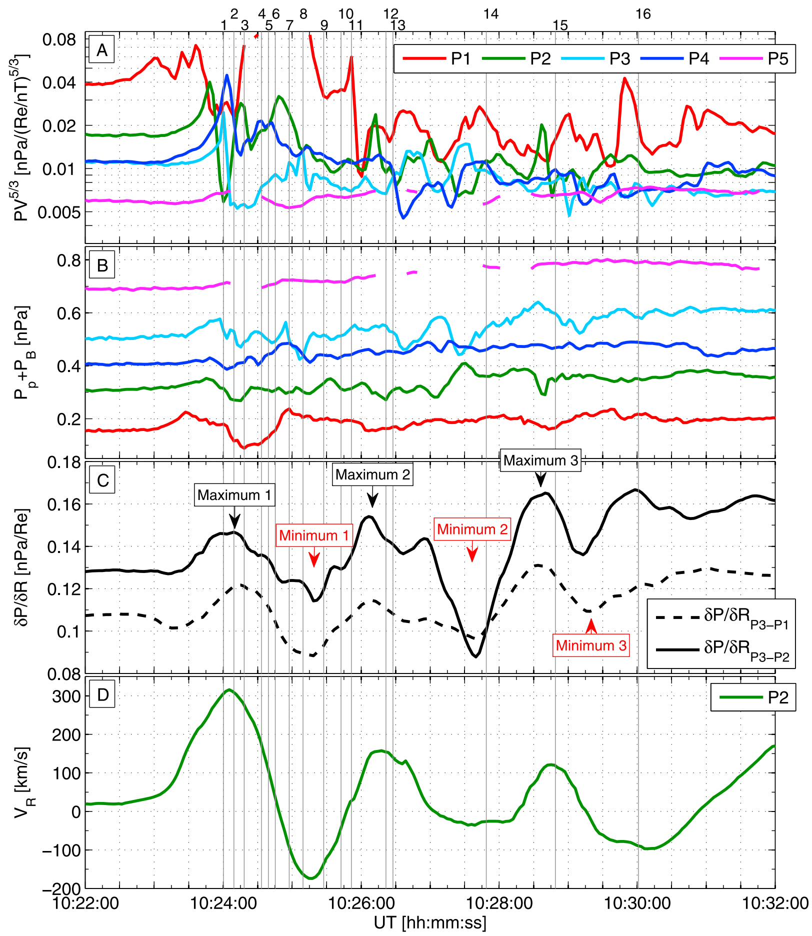

Figure 2. Data from five THEMIS spacecraft on 17 March 2008 between 10:22 and 10:32 UT: (a) local flux tube entropy $PV^{5/3}$, for which the flux tube volume V was calculated using formula (6) of *Wolf et al.* [2006]; (b) sum of plasma and magnetic pressure; (c) radial pressure gradient $\delta P/\delta R$ between P3 and P1 (dashed line), and between P3 and P2 (solid line), and (d) radial velocity component for spacecraft P2 with positive values in the Earth's direction. Data in Figures 2c and 2d were averaged over a 45-second-long window sliding with a 3-second step. See legends for color coding.

$\delta P/\delta R$, it confirmers the above suggestion that the bubble has recoiled tailward. Just before 10:26:27 UT, the pressure gradient increased again (Maximum 2). The second increase was followed by another decrease (Minimum 2) around 10:27:48 UT. Around 10:28:48 UT $\delta P/\delta R$ enhanced for the third time (Maximum 3) and then depleted again (Minimum 3, around 10:29:15 UT). Appearance of the minima in $\delta P/\delta R$ probably means, that the earthward moving flow burst stopped and recoiled tailward three times.

[12] Probe P2 was located equidistant between P1 and P3, and observed the major behavior of the bubble bouncing in the radial direction. Figure 2d depicts the radial component of the plasma velocity V_R at the location of P2. In order to suppress high-frequency fluctuations in V_R we averaged its value the same way as the $\delta P/\delta R$ data. One can see that V_R behaves like a damped sine function: $V_R(t) = V_0 \exp(-\alpha t)\sin(\frac{2\pi}{T}t)$, with the period of oscillation T of about 140 seconds and the damping factor α on the order of 0.5. One can also estimate that the spatial scale of the oscillation exceeded the distance between P1 and P3, i.e. 3 Re. While the earthward flows ($V_R > 0$) correspond to the enhanced pressure gradients, the tailward flows ($V_R < 0$) correspond to the depleted pressure gradients.

[13] Figure 3 shows selected sequential snapshots of the plasma velocity field in the (X, Y) GSM plane as observed by THEMIS between 10:24:00 and 10:30:01 UT. The snapshots are numbered at the top. The initial configuration of the plasma sheet magnetic field lines, predicted by the AM-01 model [*Kubyshkina et al.*, 2009], is shown in the first snapshot. See also Animation S1 containing all the snapshots (see auxiliary material).[1]

[14] Snapshot 2 in Figure 3 shows the moment when the BBF reached the shortest distance to the Earth around 10:24:09 UT. The flow velocity field observed by P1 (red), P2 (green) and P4 (blue) reveals a vortex (indicated by a solid circle with arrows pointing counterclockwise). Further, snapshots 3 to 10, between 10:24:18 UT and 10:25:42 UT, show that the plasma flow changed direction tailward. The velocity vectors, originating from the positions of P2 (green) and P4 (blue) spacecraft, rotated symmetrically through the dusk (P2) and dawn (P4) sides of the plasma sheet. In snapshot 6, at 10:24:45 UT, the two vectors rotated tailward and faced the oppositely directed flow, still observed by P1 (red). Then, snapshots 7 through 10, between 10:24:57 UT

[1] Auxiliary materials are available in the HTML. doi:10.1029/2009GL041971.

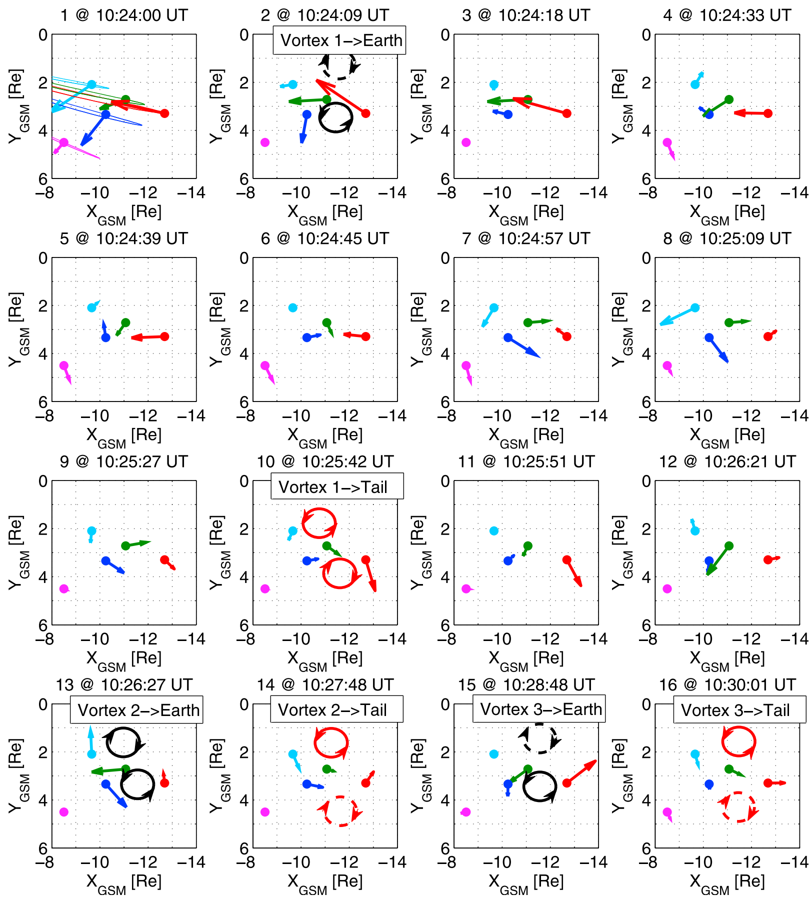

Figure 3. Selected sequential snapshots of the plasma velocity field in the (X, Y) GSM plane inside a plasma sheet during BBF passage as observed by five THEMIS spacecraft. The snapshots are numbered from left to right and from top to bottom. Times are shown above the snapshots and marked as in Figures 1 and 2 by grey vertical lines. The initial magnetic field lines configuration is overplotted in the first snapshot as predicted by the adapted Tsyganenko 96 model [*Kubyshkina et al.*, 2009]. See also a movie containing all the snapshots (attached to the article as auxiliary material).

and 10:25:42 UT, show that while the flow velocity remained tailward at P2 and P4, the flow at P1 changed its direction from earthward to tailward as well.

[15] In snapshot 10 of Figure 3 the flow velocity field observed by P1 (red), P2 (green), and P4 (blue) reveals a vortex (indicated by a solid circle with arrows pointing clockwise) with the sense of rotation, which is opposite to that in snapshot 2. In addition, the observations of P3 (cyan) suggest that there might have been observed the second vortex rotating counterclockwise (indicated by a solid circle with arrows pointing counterclockwise).

[16] Finally, snapshots 11 through 13, between 10:25:51 UT and 10:26:27 UT show just an opposite behavior of the velocity field to what was observed in snapshots 3 through 10, between 10:24:09 UT and 10:25:42 UT. In snapshot 13, at 10:26:27 UT one can see that the two vortices have changed their sense of rotation (compare with snapshot 10). The dusk side of the velocity field in snapshot 13 is similar to the one in snapshot 2. It may well be that, at 10:24:09 UT (snapshot 2 in Figure 3) all the spacecraft were located duskward from the flow burst and hence were unable to observe the second vortex located at its dawn side. We show the possible location of the second vortex by a dashed circle with arrows pointing clockwise.

[17] Snapshots 2 and 13 of Figure 3, which show the vortical patterns created by the earthward moving flow bursts, correspond to the enhanced pressure gradients (Maxima 1 and 2 in Figure 2). However, the vortical pattern in snapshot 10 of Figure 3, which was created by the tailward moving flow burst, was observed when the pressure gradient depleted (Minimum 1 in Figure 2). Further, snapshots 14, 15, and 16 of Figure 3 show the vortical patterns which were observed around the other moments of enhanced and depleted radial pressure gradients, which are indicated in Figure 2e (Minimum 2, Maximum 3, and Minimum 3). The vortical patterns, observed in snapshots 2, 10, 13, 14, 15, and 16 were roughly equidistant in time (70 seconds on average).

3. Discussion

[18] The process of the BBF overshooting and its following rebound was recently investigated in detail with the help of similar THEMIS observations on 17 March 2008 around 9:12 UT [*Panov et al.*, 2010]. They showed that after the BBF stopped moving earthward the enhanced radial pressure gradients could push the plasma flows then tailward. In this letter we demonstrate multiple overshoot and rebound of

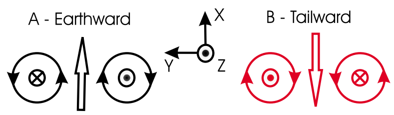

Figure 4. Sketch illustrating formation of two vortices by a flow burst moving (a) earthward and (b) tailward in the plasma sheet. The direction of the field-aligned currents are shown by dots (northward) and crosses (southward).

a BBF, whose braking was accompanied by interlaced enhancements and depletions of radial pressure gradients.

[19] The damped oscillation of a low-entropy filament about its equilibrium position manifests itself directly through the damped-sine-like trace of the radial velocity in the center of the BBF funnel (see Figure 2d). There are also ground-based observations (not shown here) that do not contradict this interpretation: The model of *Kubyshkina et al.* [2009] revealed that the footprints of the magnetic field lines, which are associated with the BBF, would be found around 70 degrees latitude and 190 degrees longitude. This area was covered by the Fort Yukon All-Sky Imager which showed three enhancements of auroral emissions around the times of the pressure gradient enhancements, whose peak luminosities decreased one after another. Also, the THEMIS ground-based magnetometer array observed Pi2 pulsations, which started with the first earthward flow burst, at a frequency corresponding to the time between the subsequent pressure enhancements, and gradually faded away. Although the above observations suggest that the damped oscillation of a low-entropy filament to be a plausible explanation of the multiple overshoot and rebound, there is still a possibility left that it was caused by three different earthward flow bursts.

[20] Damped oscillation of BBFs about their equilibrium position was predicted by *Chen and Wolf* [1999] with the help of a 2D MHD model. 3D modeling [*Birn et al.*, 2004] and observations [*Keika et al.*, 2009; *Keiling et al.*, 2009; *Panov et al.*, 2010] have revealed that the possibility for a plasma to move in the azimuthal direction allows vortex formation. We found that the earthward and tailward flow bursts form vortices with opposite sense of rotation. Figure 4 illustrates formation of the vortices during the earthward (Figure 4a) and the tailward (Figure 4b) flow bursts. Figure 4a is similar to that of *Birn et al.* [2004, Figure 19]. Figure 4b shows that the tailward-directed flow burst forces the vortices on the two sides of the BBF funnel to change their sense of rotation. Indeed, numerical 3D MHD simulations revealed presence of both configurations during the oscillatory BBF braking (J. Birn, private communication, 2009). Hence, the field-aligned currents of region-1, generated by the vortices [*Birn et al.*, 2004] are flowing in the opposite directions during the earthward- and the tailward-directed flow bursts. Therefore, the results of this analysis are important for understanding of the magnetosphere-ionosphere coupling phenomena.

[21] **Acknowledgments.** We acknowledge NASA contract NAS5-02099 for use of data from the THEMIS Mission. Specifically: U. Auster for the use of FGM data provided under the lead of the Technical University of Braunschweig and with financial support through the German Ministry for Economy and Technology and the German Center for Aviation and Space (DLR) under contract 50 OC 0302; C. W. Carlson for use of ESA data; R. P. Lin for use of SST data. For the GBO/ASIs we acknowledge S. Mende and E. Donovan, NASA contract NAS5-02099 and the CSA for logistical support in fielding and data retrieval from the GBO stations. We thank M. Kubyshkina for assisting us with their model. We highly appreciate discussions with J. Birn and V. A. Sergeev.

References

Angelopoulos, V. (2008), The THEMIS mission, *Space Sci. Rev.*, *141*, 5–34, doi:10.1007/s11214-008-9336-1.
Angelopoulos, V., W. Baumjohann, C. F. Kennel, F. V. Coroniti, M. G. Kivelson, R. Pellat, R. J. Walker, H. Lühr, and G. Paschmann (1992), Bursty Bulk flows in the inner central plasma sheet, *J. Geophys. Res.*, *97*, 4027–4039.
Angelopoulos, V., C. F. Kennel, F. V. Coroniti, R. Pellat, M. G. Kivelson, R. J. Walker, C. T. Russell, W. Baumjohann, W. C. Feldman, and J. T. Gosling (1994), Statistical characteristics of bursty bulk flow events, *J. Geophys. Res.*, *99*, 21257–21280.
Angelopoulos, V., et al. (1996), Multipoint analysis of a bursty bulk flow event on April 11, 1985, *J. Geophys. Res.*, *101*, 4967–4989.
Auster, H. U., et al. (2008), The THEMIS fluxgate magnetometer, *Space Sci. Rev.*, *141*, 235–264, doi:10.1007/s11214-008-9365-9.
Baumjohann, W., G. Paschmann, and H. Lühr (1990), Characteristics of High-Speed Ion Flows in the Plasma Sheet, *J. Geophys. Res.*, *95*, 3801–3809.
Baumjohann, W., G. Paschmann, T. Nagai, and H. Lühr (1991), Superposed epoch analysis of the substorm plasma sheet, *J. Geophys. Res.*, *96*, 11,605–11,608, doi:10.1029/91JA00775.
Baumjohann, W., M. Hesse, S. Kokubun, T. Mukai, T. Nagai, and A. A. Petrukovich (1999), Substorm dipolarization and recovery, *J. Geophys. Res.*, *104*, 24,995–25,000, doi:10.1029/1999JA900282.
Birn, J., J. Raeder, Y. Wang, R. Wolf, and M. Hesse (2004), On the propagation of bubbles in the geomagnetic tail, *Ann. Geophys.*, *22*, 1773–1786.
Chen, C. X., and R. A. Wolf (1999), Theory of thin-filament motion in Earth's magnetotail and its application to bursty bulk flows, *J. Geophys. Res.*, *104*, 14,613–14,626, doi:10.1029/1999JA900005.
Goertz, C. K., and W. Baumjohann (1991), On the thermodynamics of the plasma sheet, *J. Geophys. Res.*, *96*, 20,991–20,998.
Hesse, M., and J. Birn (1991), On dipolarization and its relation to the substorm current wedge, *J. Geophys. Res.*, *96*, 19,417–19,426, doi:10.1029/91JA01953.
Keika, K., et al. (2009), Observations of plasma vortices in the vicinity of flow-braking: A case study, *Ann. Geophys.*, *27*, 3009–3017.
Keiling, A., et al. (2009), Substorm current wedge driven by plasma flow vortices: THEMIS observations, *J. Geophys. Res.*, *114*, A00C22, doi:10.1029/2009JA014114.
Kubyshkina, M., V. Sergeev, N. Tsyganenko, V. Angelopoulos, A. Runov, H. Singer, K. H. Glassmeier, H. U. Auster, and W. Baumjohann (2009), Toward adapted time-dependent magnetospheric models: A simple approach based on tuning the standard model, *J. Geophys. Res.*, *114*, A00C21, doi:10.1029/2008JA013547.
McFadden, J. P., C. W. Carlson, D. Larson, V. Angelopoulos, M. Ludlam, R. Abiad, B. Elliot, P. Turin, and M. Marckwordt (2008), The THEMIS ESA plasma instrument and in-flight calibration, *Space Sci. Rev.*, *141*, 277–302.
Nakamura, R., et al. (2004), Spatial scale of high-speed flows in the plasma sheet observed by Cluster, *Geophys. Res. Lett.*, *31*, L09804, doi:10.1029/2004GL019558.
Panov, E. V., et al. (2010), Plasma sheet thickness during a bursty bulk flow reversal, *J. Geophys. Res.*, doi:10.1029/2009JA014743, in press.
Sergeev, V. A., V. Angelopoulos, J. T. Gosling, C. A. Cattell, and C. T. Russell (1996), Detection of localized, plasma-depleted flux tubes or bubbles in the midtail plasma sheet, *J. Geophys. Res.*, *101*, 10,817–10,826, doi:10.1029/96JA00460.
Shiokawa, K., W. Baumjohann, and G. Haerendel (1997), Braking of high-speed flows in the near-Earth tail, *Geophys. Res. Lett.*, *24*, 1179–1182, doi:10.1029/97GL01062.
Volwerk, M., K.-H. Glassmeier, A. Runov, R. Nakamura, W. Baumjohann, B. Klecker, I. Richter, A. Balogh, H. Rème, and K. Yumoto (2004), Flow burst-induced large-scale plasma sheet oscillation, *J. Geophys. Res.*, *109*, A11208, doi:10.1029/2004JA010533.
Wolf, R. A., V. Kumar, F. R. Toffoletto, G. M. Erickson, A. M. Savoie, C. X. Chen, and C. L. Lemon (2006), Estimating local plasma sheet $PV^{5/3}$ from single-spacecraft measurements, *J. Geophys. Res.*, *111*, A12218, doi:10.1029/2006JA012010.

V. Angelopoulos, Institute of Geophysics and Planetary Physics, University of California, 3845 Slichter Hall, Los Angeles, CA 90095, USA.
W. Baumjohann, R. Nakamura, E. V. Panov, A. Retinò, and M. Volwerk, Space Research Institute, Austrian Academy of Sciences, Schmiedlstraße 6, A-8042 Graz, Austria. (evgeny_panov@mail.ru)

K.-H. Glassmeier, Institut für Geophysik und Extraterrestrische Physik, Technische Universität Braunschweig, Mendelssohnstr. 3, D-38106 Braunschweig, Germany.

D. Larson and J. P. McFadden, Space Science Laboratory, University of California, 7 Gauss Way, Berkeley, CA 94720, USA.

T. Takada, Institute of Space and Astronautical Science, JAXA, Yoshinodai 3-1-1, Sagamihara 229-8510, Japan.

A. A. Petrukovich, Space Research Institute, Russian Academy of Sciences, 84/32 Profsoyuznaya St., 117997 Moscow, Russia.